INTER-ELEMENT COUPLING EFFECTS IN PULSE-ECHO ULTRASONIC FINGERPRINT SENSORS

Xiaoyue Jiang[1], Hao-Yen Tang[1], Yipeng Lu[2], Eldwin J. Ng[3], Julius M. Tsai[3], Michael J. Daneman[3], Bernhard E. Boser[1], and David A. Horsley[2]

[1]Univeristy of California, Berkeley, CA, USA

[2]Univeristy of California, Davis, CA, USA

[3]Invensense Inc., San Jose, CA, USA

ABSTRACT

Ultrasonic fingerprint sensors based on micromachined ultrasound transducers require very fine pitch to achieve high resolution imaging. We investigate a 110×56 PMUT array based on monolithic eutectic bonding to CMOS. To achieve high fill-factor, the PMUTs are anchored through small eutectic pillars, resulting in a high degree of mutual coupling between neighboring PMUTs. As a result, the mode shape is more complicated than a single-MUT dynamic model. We created a finite element model that better models the mode shapes exhibited by the entire array. Experimental measurement of the mode-shape via laser Doppler vibrometry allows us to compute the volume velocity, which correlates to the measured far field pressure.

INTRODUCTION

To meet the 500 DPI resolution standard for fingerprint sensors in consumer electronics, ultrasonic fingerprint sensors based on micromachined ultrasound transducers (MUTs) require a dramatic reduction in the PMUT size to < 50µm. However, when the spacing between MUTs is small, cross-talk from mechanical and acoustical coupling is greatly increased [1,2]. Consequently, the sensor's pulse-echo performance is not accurately modeled using single-MUT dynamic models. Instead the array dynamics must be understood. Here, we investigate a 110×56 piezoelectric MUT (PMUT) array based on monolithic AlGe eutectic bonding of a PMUT wafer to a CMOS wafer [3]. To achieve high (>50%) fill-factor, the PMUTs are anchored through small AlGe pillars, resulting in a high degree of mutual coupling between neighboring PMUT cells as well as displacement outside the designed PMUT region. We developed a finite-element method (FEM) model of the array that captures the array's fundamental mode shapes. Scanning laser Doppler vibrometry (LDV) was used to experimentally measure the mode-shape when the array is immersed in fluid, allowing us to compute the volume velocity at two different frequencies of operation. The resulting volume velocity allows the transmit pressure to be predicted and compared with experimental pressure measurements.

DESIGN

A cross-section schematic of an individual PMUT is shown along with photographs of the 110×56 sensor chip in Figure 1. Each PMUT is a piezoelectric unimorph composed of 1 µm thick AlN on a single-crystal silicon layer with 1.7 µm nominal thickness. Al-Ge eutectic bonds on SiO_2 standoffs provide the mechanical anchor and electrical contact to the PMUT [4]. The PMUTs are formed on an SOI MEMS wafer that is bonded to a CMOS wafer. Following wafer bonding, the MEMS handle wafer is mechanically thinned to 200 µm thickness and the PMUT array is exposed by through-wafer DRIE etch that removes the MEMS handle wafer in a 4.64 mm by 3.36 mm region at the center of each 5.36 by 4.58 mm die. The array consists of 43 µm x 30 µm PMUTs on a 43 µm x 58 µm grid, resulting in a resolution of 591 x 438 DPI. As shown in Figure 1, the PMUTs in the same column are separated by 28 µm x 30 µm SiO_2 anchors. The spacing between anchors defines the 30 µm vertical dimension of the PMUT, while the horizontal dimension of the PMUT is equal to the 43 µm column pitch. To increase the fill-factor, there are no anchors between PMUTs in adjacent columns, but the AlN layer is removed between columns to reduce mechanical coupling. The fact that there are no anchors between the columns, and the presence of unsupported AlN/Si membrane between the anchors of neighboring columns is the main origin of the mechanical cross-talk behavior observed in the experiments reported here.

A 0.18 µm CMOS wafer with 24V high-voltage transistors provides signal-processing electronics, described in detail in [5]. Each of the 6,160 PMUTs in the array has a dedicated receive (RX) amplifier that is connected to the Al top electrode during the receive phase. The 56 PMUTs in each column share a common Mo bottom electrode that is connected to a 24V transmit amplifier (TX) during the transmit phase. To protect the RX amplifier from the high TX voltage signal, a TX/RX switch connects each top electrode to ground (GND) during transmit.

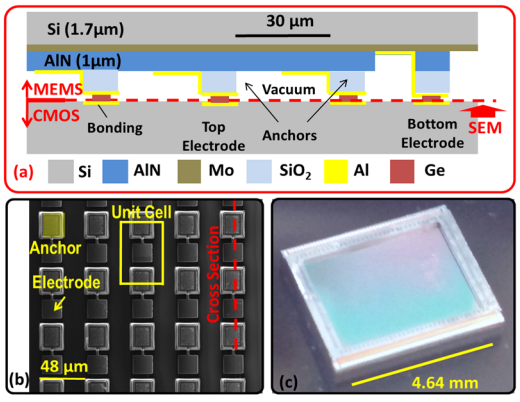

Figure 1: Fingerprint sensor diagrams: (a) schematic cross-section of 3 PMUTs and the contact to the Mo bottom electrode; (b) SEM image of the PMUT array, viewed from the top electrode side after debonding from CMOS; (c) photograph of the 4.6 mm by 3.2 mm sensor.

MECHANICAL MODEL

To model the transmit-receive behavior of the array, we begin with the connection between vibration amplitude and acoustic pressure. The theoretical surface pressure of a PMUT unit cell p_0 is given by the product of the volume velocity V_v and the acoustic impedance of the surrounding medium Z_f,

$$p_0 = V_v Z_f \quad (1)$$

The volume velocity is the average velocity of the unit cell multiplied by the area, A, which we write as

$$V_v = 2\pi f_0 d_{eff} A \quad (2)$$

where f_0 is the vibration frequency and $d_{eff} = \iint d_i dA/A$ is the average displacement over the unit cell.

To predict the value of d_{eff} at a given excitation frequency, we created a finite element method (FEM) simulation. The first four mode-shapes and their corresponding undamped natural frequencies are shown in Figure 2. The 31 MHz mode-shape exhibits the expected shape, where the dominant vibration amplitude occurs beneath the top electrode of each PMUT in the array. The other modes exhibit unanticipated behavior: at 17 MHz most motion occurs in the space between PMUTs in adjacent columns; at 34 MHz the entire region between columns vibrates; and at 41 MHz, the un-electroded space between anchors vibrates.

To identify the mode that produces the largest surface pressure, we then simulated the volume velocity of an immersed array as a function of input frequency. The simulated volume velocity in response to a 1 V sinusoidal input with varying frequency is shown in Figure 3, along with the mode-shapes corresponding to the two peaks at 14.75 MHz and 19.25 MHz. The immersed mode-shape at 14.75 MHz resembles the undamped mode-shape at 34 MHz, whereas the 19.25 MHz response appears to be a combination of modes. Note that the peak amplitude at the center of each PMUT is much larger at 14.75 MHz than it is at 19.25 MHz (0.41 nm/V versus 0.17 nm/V). However, there is significant anti-phase vibration in the region between columns, reducing the total volume velocity of both modes.

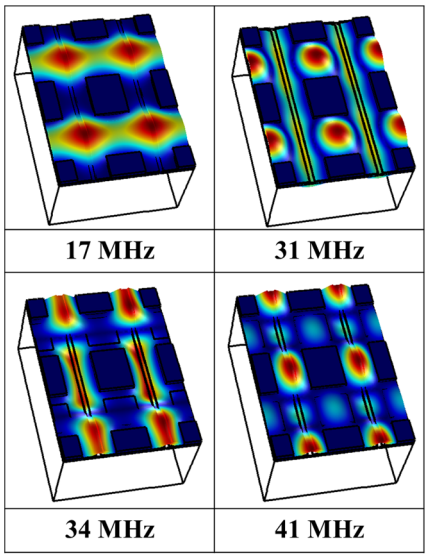

Figure 2: FEM simulated mode-shapes of the PMUT array, viewed from the top electrode side. The simulated area includes two PMUTs in the same column, separated by a SiO_2 anchor (blue rectangle) at the center. The vertical bars between the columns show the region where the AlN layer is removed.

EXPERIMENTAL RESULTS

PMUTs were measured in fluid (Fluorinert FC-70, 3M) using a Laser Doppler Vibrometer (LDV, UHF-120, Polytec, Inc.) with a precision xy positioning stage. The full-field, time-domain vibration of the PMUT array in response to pulsed inputs was measured with a 4 µm scanning grid. During the experiment, the laser was focused on the PMUT plane and the refractive index of FC-70 is used to correct the measured amplitude. Limited by the CMOS design, 24V pulsed inputs at 14 MHz and 20 MHz were used to drive five columns of PMUTs. The measured mode shape of 5 columns of PMUTs excited with a 2 cycle 14 MHz pulse input is shown in Figure 4. The time-domain displacement at three characteristic locations, PMUT center (A), between PMUT columns (B), and between PMUT rows (C), are plotted to show their different decay envelopes and frequencies. At 14 MHz, the displacements at points A and B have opposite phase. The mode shape and phase difference agree well with the FEM simulations shown in Figure 3. In addition, the magnitude of the displacement at point A is consistent with the simulation at 14 MHz input, where a peak displacement of 0.16 nm/V is predicted.

The measured mode shape of 5 columns of PMUTs

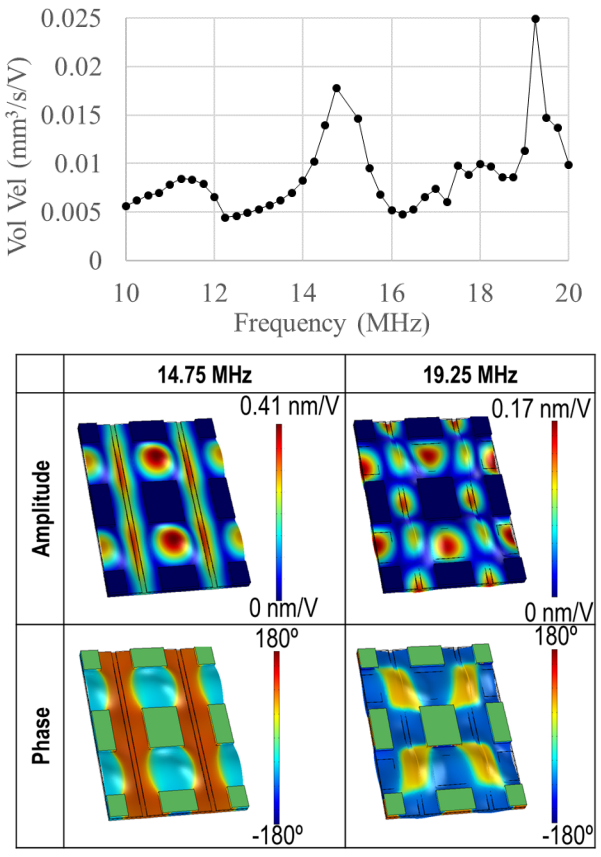

Figure 3: Simulated volume velocity response with a 1 Volt input (top). Amplitude and phase mode-shapes observed at the frequencies with peak volume velocity (bottom).

excited with a 2 cycle 20 MHz pulse input is shown along with the time-domain displacement and volume velocity plots in Figure 5. The displacement at point A is in-phase with point C, but antiphase with point B. The mode shape and phase difference are as modeled in simulation. In addition, the magnitude of the displacement at point A is consistent with the peak displacement of 0.12 nm/V predicted by FEM. Comparing the results in Figure 4 and Figure 5, the peak displacement at the PMUT center at 14 MHz input is twice that at 20 MHz input. Moreover, the ring-down times are different at the two different frequencies. A shorter ring-down will lead to higher axial resolution, since the axial resolution AR scales as

$$AR \sim \lambda(N_t + N_r)/2 \quad (3)$$

where λ is the radiating wavelength, N_t is the number of input pulse, and N_r is the number of ring down pules. N_r linearly scales with the quality factor Q [6]. Since the immersed Q is determined by the mode's acoustic radiation, we attribute the difference in ring-down time of the two modes to a difference in the acoustic radiation of these modes.

The mode-shapes measured via scanning LDV allow the volume velocity to be computed. The volume velocity computed from the mode shapes is 0.033 mm^3/s at 14 MHz and 0.028 mm^3/s at 20 MHz. Note that the volume velocities are similar despite the fact that the peak displacements differ by a factor of 2. Comparing to the FEM model shown in Fig. 3, the predicted volume velocity with a 24V input is 0.096 mm^3/s at 14 MHz (~3x greater than the experimental result) and 0.12 mm^3/s at 20 MHz (~4x greater than the experimental result). Some of the difference between experiment and model is due to fabrication variation and some is due to the fact that the pulsed input used in experiments does not produce the full steady-state amplitude. We note that both modes suffer from reduced volume velocity due to anti-phase motion between the columns. For comparison, the volume velocity predicted using a simple model based on a single circular PMUT with the same area is 0.073 mm^3/s at 14 MHz (2.2x greater than the experiment) and 0.05 mm^3/s at 20 MHz (1.8x greater than the experiment).

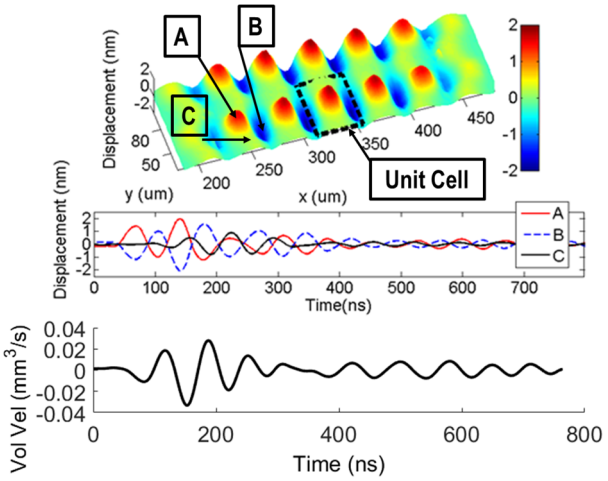

Figure 4: Top: measured TX mode shape following 2 cycle 14 MHz pulse input. Bottom: time-domain displacement at PMUT center (A), between PMUT columns (B), and between rows (C). Bottom: computed volume velocity of a unit cell.

The pressure of the TX pulse was measured using a 40 µm diameter hydrophone (Precision Acoustics) at a distance 800 µm away from the array. The measured TX pressure wave, shown in Figure 6, has a peak pressure of 9.0 kPa at 14 MHz and 7.1 kPa at 20 MHz when 5 columns were excited with a 2-cycle pulse. To compare this with the pressure predicted from the volume velocity computed from the measured mode-shapes, we relate the theoretical surface pressure to the pressure at a distance r from the array by summing the effective PMUTs with a pulsed input:

$$p(r) \sim \sum p_0 R_0 r^{-1} \quad (4)$$

where $R_0 = S/\lambda$ is the Rayleigh distance for a source with surface area S radiating at an acoustic wavelength λ. Using the area of one PMUT cell, the Rayleigh distance for a single PMUT unit cell is 25 µm at 14 MHz and 35 µm at 20 MHz. Substituting the volume velocities computed from the LDV measurements into the surface pressure equation (1), the theoretical surface pressure is 33kPa at 14 MHz and 28kPa at 20 MHz for one PMUT unit cell. Substituting these surface pressures into equation (4) and accounting for the pulsed operation, the expected pressure at 0.8 mm from the array is about 10 kPa at 14MHz and 12 kPa at 20 MHz, close to the values measured with the hydrophone.

The performance of the array at 14 MHz and 20 MHz is summarized in Table 1 which shows the measured peak displacement d_p, computed volume velocity V_v from LDV mode-shape, pressure calculated from the mode-shape p_c, and measured pressure output p_m. Note that the volume velocities of the two modes are quite similar, because the ratio of the displacement amplitudes (2:1) is almost the inverse of the frequency ratio (14:20) of the two modes. As a result, the TX pressure is roughly the same from both

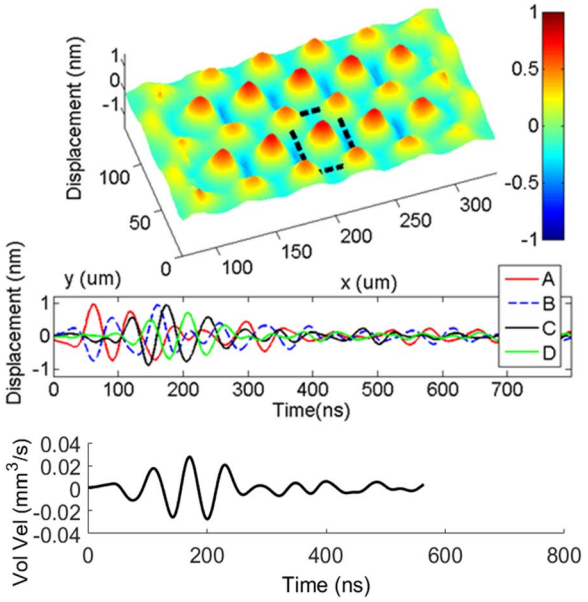

Figure 5: Top: measured TX mode shape following 2 cycle 20 MHz pulse input. middle: time-domain displacement at PMUT center (A), between PMUT columns (B, C), and between rows (D). Each point exhibits different decay envelopes and frequencies. Bottom: computed volume velocity of a unit cell.

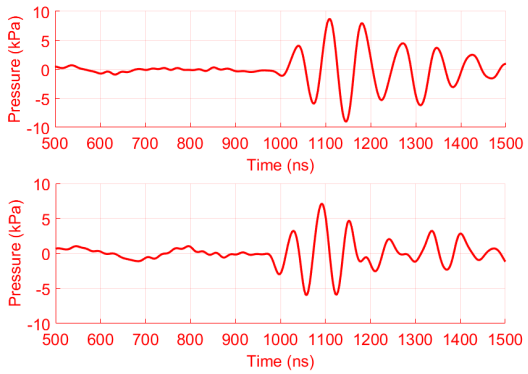

Figure 6: Measured pressure in response to 14 MHz (top) and 20 MHz (bottom) pulse inputs.

modes. While the model predicts slightly higher TX pressure from the 20 MHz mode than the 14 MHz mode and the experiment shows the opposite result, the difference is within the measurement error due to uncertainties in position of the hydrophone.

Table 1: Performance summary

Mode	d_p	V_v	Computed p_c	Hydrophone p_m
14 MHz	2 nm	0.033 m^3/s	10 kPa	9 kPa
20 MHz	1 nm	0.028 m^3/s	12 kPa	7.1 kPa
Ratio	2	1.2:1	0.8	1.3

CONCLUSION

This paper studied the mechanical behavior of a 56x110 array PMUT ultrasonic fingerprint sensor. Using FEM models, we have shown there are two distinct deflection of motion at different input frequency. However, the pressure output from the two deflection of motion are compatible. Moreover, significant vibration occurs in regions between the PMUTs. Because this vibration is in antiphase with the vibration of the PMUTs, the volume velocity is reduced by roughly a factor of two relative to the value that would be predicted from the PMUT motion alone. We have verified that the measured TX pressure is in reasonable agreement with the value predicted from the LDV-measured volume velocity, leading us to conclude that the TX performance could be improved by a factor of two or more through improved mechanical design. Because a PMUT is a reciprocal transducer, improvements to TX performance usually produce an equal increase in RX performance, suggesting that the improved design could achieve a 4-fold increase in pulse-echo signal-to-noise ratio.

ACKNOWLEDGEMENTS

The authors thank InvenSense Inc. for access to instruments for testing.

REFERENCES

[1] K. K. Park and B. T. Khuri-Yakub, "Dynamic response of an array of flexural plates in acoustic medium," *J. Acoust. Soc. Amer.*, vol. 132, pp. 2292-2303, 2012.

[2] S. H. Wong, M. Kupnik, X. Zhuang, D. Lin, K. Butts-Pauly, and B. T. Khuri-Yakub, "Evaluation of waver bonded CMUTs with rectangular membranes featuring high fill factor," *IEEE Trans. Ultrason. Ferroelectr. Freq. Control*, vol. 55, no. 9, pp. 2053-2065, Sep. 2008.

[3] X. Jiang, H.Y. Tang, Y. Lu,, X. Li, J.M. Tsai, M. Daneman, . Boser, D.A. Horsley, "Monolithic 591×438 DPI ultrasonic fingerprint sensor," *2016 IEEE MEMS*, Shanghai, 2016, pp. 107-110.

[4] J.M. Tsai, M. Daneman, B. Boser, D.A. Horsley, M. Rais-Zadeh, H.Y. Tang, Y. Lu, O. Rozen, A.F. Liu, and F. Assaderaghi, "Versatile CMOS-MEMS integrated piezoelectric platform," *Transducers*, 2015 pp. 2248-2251

[5] H. Y. Tang, Y. Lu, X. Jiang, E.J. Ng, J. M. Tsai, D.A. Horsley, B. E. Boser, "3-D Ultrasonic Fingerprint Sensor-on-a-Chip" *IEEE Journal of Solid-State Circuits,* vol. 51, no. 11, 2016

[6] L. Kinsler, "Fundamentals of Acoustics," New York: Wiley, 1962

CONTACT

*X. Jiang, tel: +15622424053; joy.jiang@berkeley.edu